International Journal of Structural Integrity

Emerald Article: Effect of arbitrary bi-material combination and bending loading conditions on stress intensity factors of an edge interface crack

Kazuhiro Oda, Xin Lan, Nao-Aki Noda, Kengo Michinaka

Effect of arbitrary bi-material combination and bending loading conditions on stress intensity factors of an edge interface crack

Kazuhiro Oda, Xin Lan, Nao-Aki Noda and Kengo Michinaka
Department of Mechanical Engineering, Kyushu Institute of Technology, Kitakyushu, Japan

Abstract

Purpose – The purpose of this paper is to compute the stress intensity factors (SIFs) of single edge interface crack for arbitrary material combinations and various relative crack lengths, and compare with those for the bonded plates subjected to tensile loading conditions. It aims to discuss the results of the shallow edge interface crack on the basis of the singular stress near the free-edge corner without the crack.

Design/methodology/approach – In this study, the SIFs of interface crack in dissimilar bonded plates subjected to bending loading conditions are analyzed by the finite element method and a post-processing technique. The use of post-processing technique of extrapolation reduces the computational cost and improves the accuracy of the obtained result.

Findings – The empirical expressions are proposed for evaluating the SIFs of arbitrary material combinations.

Originality/value – Empirical functions can be used to obtain the SIFs for arbitrary material combinations for the bending loading conditions easily. It is very convenient for engineering application.

Keywords Stress intensity factor, Single-edge interface crack, Bending loading condition, Stress (materials), Physical properties of materials, Loading (physics)

Paper type Research paper

1. Introduction

Fatigue cracks are normally observed around the weld region in joints and areas of discontinuities due to the bending and welding residual stresses. The presence of cracks affects a structure's performance, and crack propagation may eventually result in the failure of a structure. The stress intensity factor (SIF) is used to predict the stress state and the stability of a crack in linear elastic fracture mechanics. Therefore, quite a lot research has been devoted to the analysis of the SIFs of crack problems.

The evaluation of the SIFs becomes complicated for the interfacial cracks due to the multiple/oscillatory singularity. Till recently, many researchers have tried to develop procedures to compute the generalized SIFs of a cracked composite structure by using analytical or numerical methods. Just mention a few of those procedures, Yuuki and Cho (1989) determined the SIFs of several interface crack problems by the boundary element method employing an extrapolation method. Miyazaki *et al.* (1993) presented the M1-integral method (an extended J-integral method) for SIF analyses of two-dimensional bimaterial interface crack problems, using the results obtained from the boundary element method. Wu (1994) presented for calculating the SIFs at the tip of

International Journal of Structural Integrity
Vol. 3 No. 4, 2012
pp. 457-475

1757-9864
DOI 10.1108/17579861211281236

an interface crack based on an evaluation of the J-integral by the virtual crack extension method. Yang and Kuang (1996) established a path independent contour integral method for the SIFs of the interface crack. Dong *et al.* (1997) proposed procedures for SIF computation using traction singular quarter-point boundary elements. Matsumto *et al.* (2000) evaluated the SIFs of bimaterial interface cracks based on the interaction energy release rates. Xuan *et al.* (2007) presented a finite element approach for finding complementary bounds of SIFs in bimaterials. The SIF is formulated as an explicit computable linear function of displacements by means of the two-point extrapolation method. Liu *et al.* (2008) developed a simple and effective numerical method to calculate the SIFs for an interface crack with one or two singularities. Treifi *et al.* (2008, 2009) computed the SIFs for different configurations of cracked/notched plates subjected to in-plane shear and bending loading conditions by the fractal-like finite element method. Noda *et al.* (2010) investigated the SIFs of the single-edge interface cracks in bonded dissimilar half-planes and finite bonded strips subjected to remote tension, and proposed a powerful empirical function for computing the SIFs of arbitrary material combinations and crack lengths. Then, Lan *et al.* (2011a, b) discussed the effect of the material combinations and the relative crack lengths to the SIFs of a single edge cracked bonded strip subjected tensile loading conditions. Although the aforementioned studies have considered the SIFs for the tensile loading conditions, Kakuno *et al.* (2010) analyzed the SIFs of edge interface crack in a bonded specimen under bending. However, the results shown by Kakuno *et al.* (2010) restrict the relative crack lengths within $a/W = 0.1 \sim 0.5$, and the SIFs of very shallow and deep interface crack have not been examined.

In this research, the improved crack tip stress method proposed by Oda *et al.* (2009), which is based on the concept of crack tip stress method introduced by Nisitani *et al.* (1999), will be used to solve the SIFs of the dissimilar bonded plates subjected to bending loading conditions and a post-processing technique of linear extrapolation will be proposed to improve the computational accuracy. The new technique reduces the computational cost significantly since very refined meshes around the crack tip are no longer necessary. The SIFs of interface crack under bending condition will be computed for arbitrary material combinations and relative crack lengths. Then, the computed results will be compared with those for the tensile loading conditions which were published previously (Noda *et al.*, 2010). Furthermore, empirical functions will also be proposed for the bending loading conditions in this paper.

2. Analysis method

2.1 Formulation for the Interface crack problems

The original crack tip stress method proposed by Nisitani *et al.* (1999) cannot be used directly into solving the interface crack problems since oscillatory singularity is observed along the interface. Then, Oda *et al.* (2009) extended this method to the interface crack problems by creating the same singularities for the reference and target unknown problems. A definition of the SIFs for an interface crack in bonded dissimilar materials was proposed by Erdogan (1965). The stress distributions along the interface are defined as shown in equation (1):

$$\sigma_y + i\tau_{xy} = \frac{K_I + iK_{II}}{\sqrt{2\pi r}} \left(\frac{r}{2a}\right)^{i\varepsilon}, \quad r \to 0 \tag{1}$$

Here, σ_y, τ_{xy} denote the stress components near the crack tip. r is the radial distance from the crack tip, and ε is the bi-elastic constant given by:

$$\varepsilon = \frac{1}{2\pi} \ln \left[\frac{((\kappa_1/G_1) + (1/G_2))}{((\kappa_2/G_2) + (1/G_1))} \right] \tag{2}$$

$$\kappa_m = \begin{cases} 3 - 4\nu_m (plane \quad strain) \\ (3 - \nu_m)/(1 + \nu_m (plane \quad stress)) \end{cases}, \quad (m = 1, 2) \tag{3}$$

where $G_m (m = 1,2)$ and $\nu_m (m = 1,2)$ are the shear moduli and poisson's ratios of either respective materials. The real and imaginary parts of the oscillatory SIFs $K_I + iK_{II}$ in equation (5) may be separated as:

$$K_I = \lim_{r \to 0} \sqrt{2\pi r} \sigma_y \left(\cos Q + \frac{\tau_{xy}}{\sigma_y} \sin Q \right) \tag{4}$$

$$K_{II} = \lim_{r \to 0} \sqrt{2\pi r} \tau_{xy} \left(\cos Q - \frac{\sigma_y}{\tau_{xy}} \sin Q \right) \tag{5}$$

and

$$Q = \varepsilon \ln \left(\frac{r}{2a} \right) \tag{6}$$

Similarly, let us consider two different interface crack problems C and D with the same crack lengths $a = a_0$ and the same combination of materials $\varepsilon = \varepsilon_0$, assuming the SIFs of problem C are given in advance and those for problem D are yet to be solved. Problem C is termed the reference problem whose values are marked with *, and problem D is termed the given unknown problem. Examining the points with the same radial distances $r = r_0$ for the two problems C and D, then gives:

$$[Q^*]_C = [Q]_D = \varepsilon_0 \ln \left(\frac{r_0}{2a_0} \right).$$

Recall equations (8) and (9), a proportional relationship given in equation (7) is established if and only if equation (8) can be satisfied:

$$\frac{[K_I]_D}{\left[K_I^*\right]_C} = \frac{\left[\sigma_y\right]_D}{\left[\sigma_y^*\right]_C} = \frac{\left[\sigma_{y,FEM}\right]_D}{\left[\sigma_{y,FEM}^*\right]_C}, \quad \frac{[K_{II}]_D}{\left[K_{II}^*\right]_C} = \frac{\left[\tau_{xy}\right]_D}{\left[\tau_{xy}^*\right]_C} = \frac{\left[\tau_{xy,FEM}\right]_D}{\left[\tau_{xy,FEM}^*\right]_C} \tag{7}$$

$$\left[\frac{\tau_{xy}^*}{\sigma_y^*}\right]_C = \left[\frac{\tau_{xy}}{\sigma_y}\right]_D \tag{8}$$

Then the SIFs of the given unknown problem (problem D) can be computed using equation (9). The condition of equation (8) can be satisfied by choosing a suitable external load for the reference problem. The detailed information about how to make the condition equation (8) satisfied by using FEM will be discussed in Section 2.2:

$$[K_I]_D = \frac{[\sigma_y]_D \left[K_1^*\right]_C}{\left[\sigma_y^*\right]_C} = \frac{[\sigma_{y,FEM}]_D \left[K_1^*\right]_C}{\left[\sigma_{y,FEM}^*\right]_C},$$
$$[K_{II}]_D = \frac{[\tau_{xy}]_D \left[K_2^*\right]_C}{\left[\tau_{xy}^*\right]_C} = \frac{[\tau_{xy,FEM}]_D \left[K_2^*\right]_C}{\left[\tau_{xy,FEM}^*\right]_C} \quad (9)$$

2.2 Determination of the reference problem and its external load

In this research, a crack along the interface of two bonded dissimilar half-planes subjected to tension and shear as shown in Figure 1(a) is treated as the reference problem. The analytical solution of the SIFs at the crack tip for the reference problem takes the following form:

$$K_I^* + iK_{II}^* = \left(\sigma_y^\infty + i\tau_{xy}^\infty\right)\sqrt{\pi a}(1 + 2i\varepsilon) \quad (10)$$

where, $\sigma_y^\infty, \tau_{xy}^\infty$ are the remote uniform tension and shear applied to the bonded dissimilar half-planes.

Using the principle of superposition, the stress components of the reference problem subjected to remote tension and shear $\sigma_y^\infty, \tau_{xy}^\infty$ can be expressed by using the values of that subjected to pure unit tension $\sigma_y^\infty = 1, \tau_{xy}^\infty = 0$ and pure

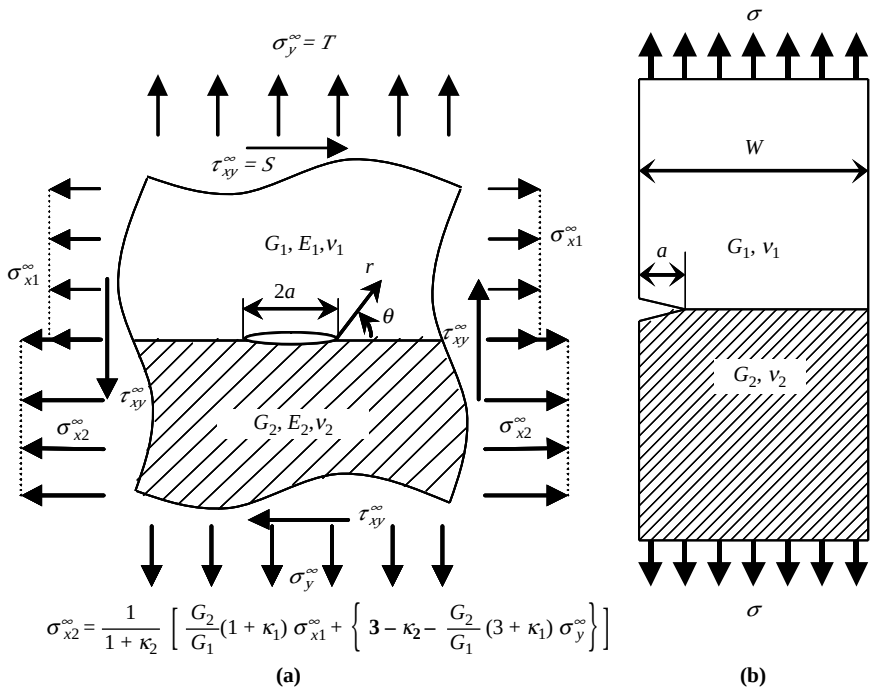

Figure 1.
Demonstration of (a) the reference problem (problem C) and (b) a given unknown problem (problem D)

unit shear $\sigma_y^{\infty}=0, \tau_{xy}^{\infty}=1$. Let $\sigma_{y0,FEM}^{*}, \tau_{xy0,FEM}^{*}$, $\sigma_{y0,FEM}^{\sigma_y^{\infty}=1,\tau_{xy}^{\infty}=0^{*}}, \tau_{xy0,FEM}^{\sigma_y^{\infty}=1,\tau_{xy}^{\infty}=0^{*}}$ and $\sigma_{y0,FEM}^{\sigma_y^{\infty}=0,\tau_{xy}^{\infty}=1^{*}}, \tau_{xy0,FEM}^{\sigma_y^{\infty}=0,\tau_{xy}^{\infty}=1^{*}}$ denote the stress components at the crack tip of the reference problem subjected to combined remote tension and shear $\sigma_y^{\infty}, \tau_{xy}^{\infty}$, pure unit tension $\sigma_y^{\infty}=1, \tau_{xy}^{\infty}=0$ and pure unit shear $\sigma_y^{\infty}=0, \tau_{xy}^{\infty}=1$, respectively. Then $\sigma_{y0,FEM}^{*}, \tau_{xy0,FEM}^{*}$ take the following form:

$$\sigma_{y0,FEM}^{*}=\sigma_{y0,FEM}^{\sigma_y^{\infty}=1,\tau_{xy}^{\infty}=0^{*}}\times\sigma_y^{\infty}+\sigma_{y0,FEM}^{\sigma_y^{\infty}=0,\tau_{xy}^{\infty}=1^{*}}\times\tau_{xy}^{\infty} \tag{11}$$

$$\tau_{xy0,FEM}^{*}=\tau_{xy0,FEM}^{\sigma_y^{\infty}=1,\tau_{xy}^{\infty}=0^{*}}\times\sigma_y^{\infty}+\tau_{xy0,FEM}^{\sigma_y^{\infty}=0,\tau_{xy}^{\infty}=1^{*}}\times\tau_{xy}^{\infty} \tag{12}$$

Recall equation (8), the FE stress components at the crack tip for the problems C and D behave:

$$\left[\frac{\tau_{xy0,FEM}^{*}}{\sigma_{y0,FEM}^{*}}\right]_C=\left[\frac{\tau_{xy0,FEM}}{\sigma_{y0,FEM}}\right]_D \tag{13}$$

where, the superscript 0 stands for the values at the crack tip. Inserting equations (11) and (12) into equation (13) gives the solution of $\tau_{xy}^{\infty}/\sigma_y^{\infty}$ needed for determining the external loads applied to the reference problem:

$$\frac{\tau_{xy}^{\infty}}{\sigma_y^{\infty}}=\frac{\sigma_{y0,FEM}\times\tau_{xy0,FEM}^{\sigma_y^{\infty}=1,\tau_{xy}^{\infty}=0^{*}}-\tau_{xy0,FEM}\times\sigma_{y0,FEM}^{\sigma_y^{\infty}=1,\tau_{xy}^{\infty}=0^{*}}}{\tau_{xy0,FEM}\times\sigma_{y0,FEM}^{\sigma_y^{\infty}=0,\tau_{xy}^{\infty}=1^{*}}-\sigma_{y0,FEM}\times\tau_{xy0,FEM}^{\sigma_y^{\infty}=0,\tau_{xy}^{\infty}=1^{*}}} \tag{14}$$

Let $\sigma_y^{\infty}=1$ so that τ_{xy}^{∞} can be determined. Inserting $\sigma_y^{\infty}=1, \tau_{xy}^{\infty}$ into equation (10) gives the values of the oscillatory SIFs for the reference problem (problem C). Finally, the SIFs for the given unknown problem (problem D) can be yielded using the proportional relationship as given in equation (15):

$$[K_I]_D=\frac{[\sigma_{y0,FEM}]_D\left[K_I^{*}\right]_C}{[\sigma_{y0,FEM}^{*}]_C},\quad [K_{II}]_D=\frac{[\tau_{xy0,FEM}]_D\left[K_{II}^{*}\right]_C}{\left[\tau_{xy0,FEM}^{*}\right]_C} \tag{15}$$

Specially, when both materials for a bonded structure are identical, all the imaginary terms in the discussion vanish. Thus, the current method is also applicable to the homogenous crack problems.

3. Numerical verification and the post-processing technique

The efficiency and accuracy of the improved crack tip stress method is demonstrated by pursuing a convergence study. The effects of the minimum element size e and the number of refined layers NL in FE analysis will be investigated and depicted through several examples.

3.1 Specifications and configurations of the FE models

The MSC.MARC 2007 r1 finite element analysis package is used to compute the stress components in this research. Figure 2(a) shows the FE model geometric configurations for the reference problem shown in Figure 1(a). The crack length for the dissimilar bonded half-planes shown in Figure 2(a) (the reference problem) is set to 2a = 20 mm. A plate width of $W = 1{,}620 \times 2a = 32{,}400$ mm and a length of $L = 2W = 64{,}800$ mm are used to model the reference problem ($L = 2W$, $W/a = 1{,}620$) since the stress components computed by FEM converge as $L > 1{,}500a$ (Oda *et al.*, 2009). Figure 2(b) shows the FE model geometric configurations for the single-edge cracked bonded strip shown in Figure 1(b) (the target unknown problem). The crack length for the target unknown problem is fixed to a = 10 mm which is the half crack length of the reference problem. The width of the bonded strip W varies from $a/W = 0.1 \sim 0.9$, the length L is assumed to be much greater than the width $W(L = 2W$ is assumed in the FE model). Furthermore, the minimum element size e of the FE models are kept the same for the reference and given unknown problems.

The singular regions around the crack tip of both the reference and the target unknown problems are well refined in a self-similar manner. Figure 2(c) shows the FE mesh type in the singular region. The element size for each inferior layer is one third of the superior one. The meshes are made of the eight-node quadrilateral elements in plane stress or plane strain conditions. Furthermore, the meshes for the reference and target unknown problems are kept the same to make sure a high computational accuracy of $\left[\tau^*_{xy}/\sigma^*_y\right]_C = [\tau_{xy}/\sigma_y]_D$.

3.2 Convergence study for the single-edge-cracked bonded strips subjected to tensile and bending loading conditions

A single edge-cracked bonded strip subjected to tension and bending loading conditions as shown in Figure 3(a) is analyzed for various crack sizes (say, $a/W = 0.1 \sim 0.9$). Figure 3(b) and (c) shows the tension applied at the top and the bottom boundaries to counter the tensile load and bending moment shown in Figure 3(a), respectively. Four pairs of models (the reference and the given unknown problems) with different minimum element sizes are tested to carry out the convergence study. The mesh

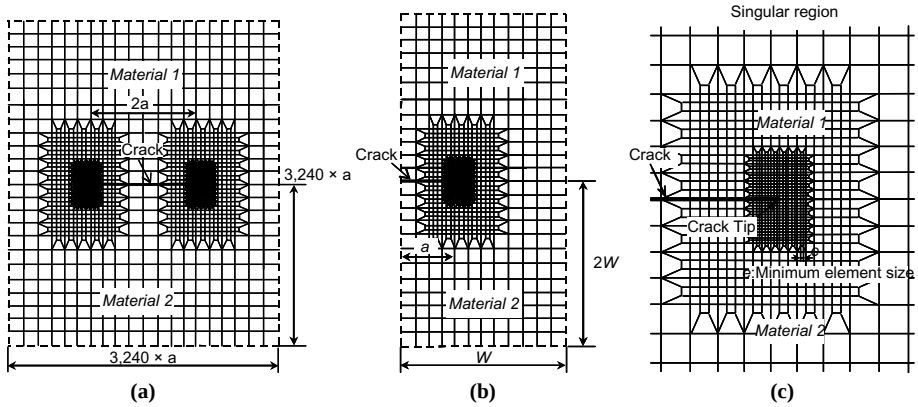

Figure 2.
FE model geometric configurations for (a) the reference problem; (b) the target unknown problem; and (c) the FE mesh in the singular region used for the analysis

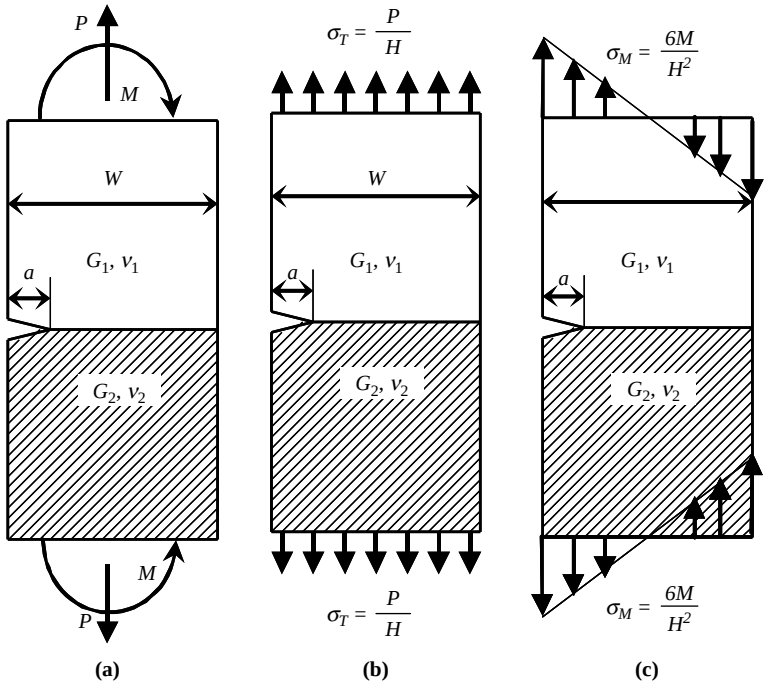

Figure 3.
(a) A single-edge-cracked bonded strip subjected to tension and bending loading conditions, tensions at the top and bottom boundaries to counter; (b) the tensile; and (c) the bending loading conditions

pattern, model density and minimum element size for each pair of models are fixed the same. Namely, the minimum element sizes for each pair of models are $a/3^5$, $a/3^6$,$a/3^7$,$a/3^8$ which corresponding to the total number of mesh layers $NL = 9, 10, 11, 12$, respectively.

The SIFs for the single-edge cracked dissimilar bonded strip $a/W = 0.8$ subjected to tensile loading conditions are plotted and compared with those of Yuuki and Cho (1989) and Miyazaki *et al.* (1993) in Figure 4. The corresponding FE stress components and other relative values in equation (15) are also tabulated in Table I for various minimum element sizes. The elastic parameters in Figure 4 and Table I are restricted to

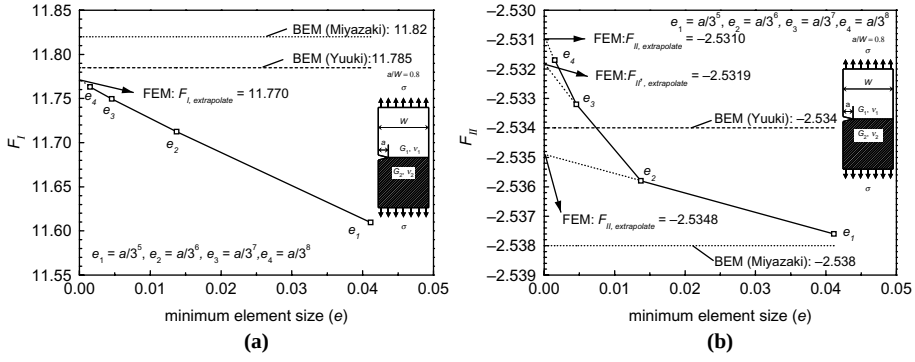

Figure 4.
Variations of normalized SIFs $F_1 = K_1/\sigma\sqrt{\pi a}$, $F_2 = K_2/\sigma\sqrt{\pi a}$ with the minimum element size e for a bonded strip (a) $a/W = 0.7$ and (b) $a/W = 0.8$ subjected to uniform tension

e	Reference problems C				Unknown problem D			Results	
	$\left[\sigma^{*}_{y0,FEM}\right]_c$	$\left[\tau^{*}_{y0,FEM}\right]_c$	$\left[F^{*}_{I}\right]_c$	$\left[F^{*}_{II}\right]_c$	$[\sigma_{y0,\ FEM}]_D$	$[\tau_{y0,FEM}]_D$	ε	$\tau^{\infty}_{xy}/\sigma^{\infty}_{y}$	$[F_I]_D$	$[F_{II}]_D$
$a/3^5$	19.3083	−3.7441	0.9891	−0.2162	226.635	−43.947	0.0679	0.0805	11.6095	−2.5376
$a/3^6$	32.4030	−7.9192	0.9893	−0.2142	383.600	−93.751	0.0679	0.0785	11.7123	−2.5358
$a/3^7$	54.0313	−16.094	0.9895	−0.2133	641.602	−191.115	0.0679	0.0776	11.7495	−2.5332
$a/3^8$	89.4632	−31.8183	0.9895	−0.2130	1063.510	−378.246	0.0679	0.0773	11.7630	−2.5317

Table I.
Tabulated results for FE models with different minimum element sizes $e(G_2/G_1 = 4v_1 = v_2 = 0.3$, Plane stress)

$E_1/E_2 = 4, \quad \nu_1 = \nu_2 = 0.3$. The data of Yuuki and Cho (1989) and Miyazaki *et al.* (1993) are plotted in dashed lines. It can be seen that increasing the number of refined layers (*NL*) can significantly improve the accuracy, however, this will lead to dramatic increase in the number of elements, and consequently the computational cost. Furthermore, Figure 4 also demonstrates that the normalized SIF $K_I/\sigma\sqrt{\pi a}$ behave linear relationship with the minimum element size. Good results can be obtained by using linear extrapolation without adding too more refined layers. Here, it should be noted that the exact values for $K_{II}/\sigma\sqrt{\pi a}$ should also be computed through linear extrapolation although a simple linear behavior is not observed for this case. Specifically, when increasing the number of refined layers $NL \rightarrow \infty$, the minimum element size $e \rightarrow 0$. Hence, the accurate SIFs for $NL \rightarrow \infty$ can be computed using the following equation:

$$K_{accu} = K^{e=0} = \frac{(e_2 K^{e1} - e_1 K^{e2})}{(e_2 - e_1)}, \quad e_1 \neq e_2 \leq \frac{a}{243} \tag{16}$$

where $K^{e=0}$ is the extrapolated SIF, and K^{e1} K^{e2} are the SIFs computed by two different meshes with the minimum element sizes e_1,e_2, respectively. According to the authors' investigation, models with the minimum element size $e = a/3^6$, $a/3^7$ are recommended since they have the best compromise between accuracy and computational cost. The normalized SIFs for other material combinations are tabulated in Table II together with those of Yuuki and Cho (1989), Miyazaki *et al.* (1993) and Matsumto *et al.* (2000). Table II illustrates that the SIF values computed by the current method are in very good agreement with those predicted by Yuuki and Cho (1989), Miyazaki *et al.* (1993) and Matsumto *et al.* (2000). Therefore, the current method can get accurate SIFs without using high model density (say, the total number of layers is $NL = 1{,}011$ in this research), and it has a faster convergence speed than other numerical methods.

The SIFs for a single-edge cracked bonded strip subjected to bending loading conditions shown in Figure 3(c) are computed and tabulated in Table III. Linear extrapolation is also employed for this case with an extremely small error. As shown in Figure 4 and Table II, the current method produced accurate results for interface crack problem under tensile loading condition. Therefore, it can be assumed that the results in Table III are also reliable.

	$K_I/\sigma\sqrt{\pi a}$				$K_{II}/\sigma\sqrt{\pi a}$			
a/W	Present	Yuuki and Cho (1989)	Miyazaki *et al.* (1993)	Matsumto *et al.* (2000)	Present	Yuuki and Cho (1989)	Miyazaki *et al.* (1993)	Matsumto *et al.* (2000)
0.1	1.209	1.201	1.209	1.199	−0.239	−0.238	−0.239	−0.237
0.2	1.368	1.387	1.368	1.368	−0.251	−0.254	−0.250	−0.251
0.3	1.653	1.653	1.654	1.655	−0.288	−0.288	−0.288	−0.288
0.4	2.100	2.100	2.101	2.102	−0.359	−0.359	−0.359	−0.358
0.5	2.805	2.807	2.807	2.806	−0.484	−0.483	−0.483	−0.483
0.6	3.998	4.000	4.006	4.001	−0.716	−0.701	−0.716	−0.714
0.7	6.284	6.298	6.304	6.298	−1.208	−1.209	−1.208	−1.204
0.8	11.768	11.785	11.820	11.780	−2.532	−2.534	−2.538	−2.515
0.9	33.735	–	–	–	−8.797	–	–	–

Table II. Normalized SIFs for the single-edge cracked bonded strips subjected to uniform tension ($G_2/G_1 = 4$, $v_1 = v_2 = 0.3$, plane stress)

Table III.
Normalized SIFs $F_1 = K_1/\sigma\sqrt{\pi a}$, $F_2 = K_2/\sigma\sqrt{\pi a}$ for a single-edge cracked bonded strip subjected to bending loading conditions shown in Figure 3(c) ($v_1 = v_2 = 0.3$, plane stress)

	$E_2/E_1 = 1$		$E_2/E_1 = 2$		$E_2/E_1 = 3$		$E_2/E_1 = 4$		$E_2/E_1 = 10$		$E_2/E_1 = 100$	
a/W	F_I	F_{II}	F_I	F_{II}	F_I	F_{II}	F_I	F_{II}	F_I	F_{II}	F_I	F_{II}
0.1	1.045	0	1.042	−0.088	1.038	−0.132	1.035	−0.159	1.025	−0.217	1.014	−0.260
0.2	1.054	0	1.052	−0.073	1.049	−0.109	1.046	−0.130	1.038	−0.176	1.029	−0.209
0.3	1.124	0	1.123	−0.070	1.121	−0.104	1.120	−0.124	1.116	−0.168	1.111	−0.198
0.4	1.261	0	1.260	−0.077	1.260	−0.115	1.259	−0.138	1.258	−0.186	1.256	−0.219
0.5	1.497	0	1.497	−0.098	1.497	−0.146	1.496	−0.175	1.496	−0.236	1.495	−0.278
0.6	1.913	0	1.912	−0.141	1.911	−0.212	1.911	−0.253	1.909	−0.343	1.907	−0.405
0.7	2.724	0	2.720	−0.238	2.716	−0.356	2.712	−0.427	2.703	−0.578	2.694	−0.687
0.8	4.673	0	4.658	−0.496	4.639	−0.743	4.625	−0.891	4.584	−1.211	4.546	−1.441
0.9	12.448	0	12.360	−1.697	12.251	−2.544	12.165	−3.050	11.921	−4.144	11.691	−4.936

4. SIFs for a shallow edge interface crack in a bonded finite strip subjected to bending loading conditions

Consider the bi-material bonded strip shown in Figure 5. It is composed of two elastic, isotropic and homogeneous strips that are perfectly bonded along the interface. The material above the interface is termed material 1, and the material below is termed material 2. The SIFs for the aforementioned problem in plane strain or plane stress are only determined on the two elastic mismatch parameters α and β. Here, the Dundurs' material composite parameters are defined as:

$$\alpha = \frac{G_1(\kappa_2 + 1) - G_2(\kappa_1 + 1)}{G_1(\kappa_2 + 1) + G_2(\kappa_1 + 1)}, \quad \beta = \frac{G_1(\kappa_2 - 1) - G_2(\kappa_1 - 1)}{G_1(\kappa_2 + 1) + G_2(\kappa_1 + 1)} \tag{17}$$

where the subscripts denote material 1 or 2, $G_m = E_m/2(1 + \nu_m)$, $(m = 1, 2)$, G_m, E_m and ν_m denote shear modulus, Young's modulus and Poisson's ratio for material m, respectively. Kolosov constant $\kappa_m = (3 - \nu_m)/(1 + \nu_m)$ for plane stress and $\kappa_m = (3 - 4\nu_m)$ for plane strain. In this research, only the SIFs for $\beta \geq 0$ in $\alpha - \beta$ space has been investigated since switching materials 1 and 2 ($mat1 \Leftrightarrow mat2$) will only reverse the signs of α and $(\beta(\alpha, \beta) \Leftrightarrow (-\alpha, -\beta))$. In this paper, we restrict our discussions to material combinations with $\beta = 0.3$ because the same phenomenon can be found from other material combinations. The SIFs are normalized using the following equation:

$$\frac{F_I = K_I}{\sigma\sqrt{\pi a}}, \quad \frac{F_{II} = K_{II}}{\sigma\sqrt{\pi a}} \tag{18}$$

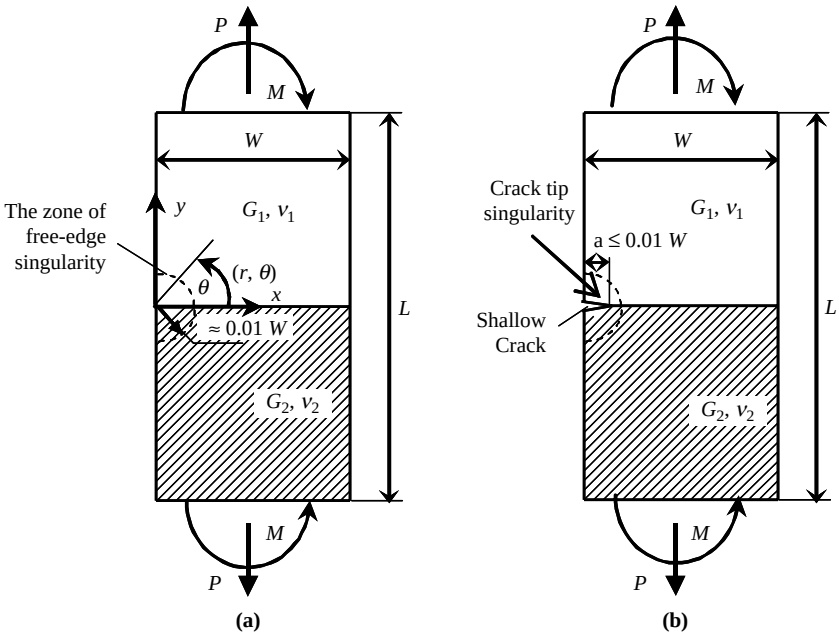

Figure 5.
(a) Free edge singularity of an un-cracked bonded strip and (b) crack tip singularity of a shallow edge interface crack in a dissimilar bonded strip

4.1 Free-edge singularity of a perfectly bonded plate

When a shallow edge interface crack initiates at the free-edge corner, the SIFs will be affected by the stress state within the zone of free-edge singularity as shown in Figure 5. The singularity at the interface corner of a bonded plate without the crack can be determined by the following relationships (Bogy, 1968, 1971):

$$\begin{aligned}
&\alpha(\alpha-2\beta)>0: \quad \lambda<1, \quad \sigma_y=\sigma_{yy}|_{\theta=0}\to\infty \quad (r\to 0) \quad \text{Singularity exist}\\
&\alpha(\alpha-2\beta)=0: \quad \lambda=1, \quad \sigma_y=\sigma_{yy}|_{\theta=0}\to \textit{finite} \quad (r\to 0) \quad \text{Uniform constant stress field}\\
&\alpha(\alpha-2\beta)<0: \quad \lambda>1, \quad \sigma_y=\sigma_{yy}|_{\theta=0}\to 0 \quad (r\to 0) \quad \text{Singularity vanish}
\end{aligned} \tag{19}$$

Let us consider a perfectly bonded dissimilar plate without crack as shown in Figure 5(a) with a cylindrical polar coordinate (r, θ) centered at the interface corner. The singular field around the interface corner can be expressed in the form Akisanya and Fleck (1997) and Chen and Nishitani (1993):

$$\sigma_\theta = Kr^{\lambda-1}f_{\theta\theta}(r,\theta), \quad \tau_{r\theta}=Kr^{\lambda-1}f_{r\theta}(r,\theta) \tag{20}$$

Here, K is the intensity of stress singularity near the corner, r is the radial distance from the corner, and λ is the index of stress singularity. And $f_{\theta\theta}(r,\theta)$, $f_{r\theta}(r,\theta)$ are angular functions of r,θ.

Many studies have considered the order of the stress singularity for bonded corners with varying geometries and material combinations (Bogy and Wang, 1971; Hein and Erdogan, 1971; Dempsey and Sinclair, 1979; Van Vroonhoven, 1992). For the bonded strip shown in Figure 5(a), the angles which the traction-free surfaces make with the interface are $\pi/2$, then the values of λ can be obtained by solving the following equation (Chen and Nishitani, 1993):

$$\begin{aligned}
D(\alpha,\beta,\lambda) = &\left[\cos^2\left(\frac{\pi}{2}\lambda\right)-(1-\lambda)^2\right]^2\beta^2+2(1-\lambda)^2\left[\cos^2\left(\frac{\pi}{2}\lambda\right)-(1-\lambda)^2\right]\alpha\beta\\
&+(1-\lambda)^2[(1-\lambda)^2-1]\alpha^2+\cos^2\left(\frac{\lambda\pi}{2}\right)\sin^2\left(\frac{\lambda\pi}{2}\right)=0
\end{aligned} \tag{21}$$

where, λ is the zero of $D(\alpha,\beta,\lambda)$ in $0<\mathrm{Re}(\lambda)<1$ that has the smallest real part. In general, $D(\alpha,\beta,\lambda)$ is expected to have several zeros in $0<\mathrm{Re}(\lambda)<1$. The values of λ for arbitrary material composite parameters (α,β) were computed in the authors' previous research (Noda *et al.*, 2010; Lan *et al.*, 2011b).

Although the order of stress singularity has been discussed in many papers, the intensity of singular stress fields has just recently been obtained (Chen and Nishitani, 1993; Reedy and Guess, 1993; Xu *et al.*, 1999). In this research, K_σ is introduced to define the intensity of singular stress in order to examine the stress field around the free-edge corner, and it is defined as:

$$K_\sigma = \lim_{r\to 0}[r^{1-\lambda}\times\sigma_{\theta|\theta=\pi/2}] \tag{22}$$

The intensity of stress singularity K for an un-cracked bonded dissimilar strip can be obtained by using (Chen and Nishitani, 1993):

$$K = K_\sigma \Big/ 4\lambda\cos(\lambda\pi/2)[(\lambda+1-\lambda\beta)\cos(\lambda\pi)+(\lambda+1)(2\lambda\beta-1)-\lambda\beta+2\lambda^2(\lambda+1)(\alpha-\beta)] \quad (23)$$

Chen and Nishitani (1993) investigated the normalized values of $K_\sigma/[(6M/W^2)W^{1-\lambda}]$ for $\lambda > 1$ for a bonded strip subjected to bending loading conditions. The values for $\lambda \leq 1$ are calculated in this research as a further work. And they are plotted in Figure 6 against material composite parameters α for $\beta = -0.2\tilde{0}.4$. It should be noted that K_τ for the shear stress component also exists but is not demonstrated here since it is negligible in magnitude comparing with K_σ. The zone of free-edge singularity domains an extent of around 0.01 times the width of the bi-material strip (Figure 5(a)). Therefore, when very shallow edge interface cracks initiate within the extent of the singular zone of bi-material bonded strips (Figure 5(b)), the SIFs will be controlled by the free edge singularity.

4.2 Variations of SIFs for the single-edge interface crack with relative crack length and material combinations

The single edge interface crack problem under the bending loading condition is calculated to examine the effect of the crack length and the material combinations on the SIFs. The double logarithmic variations of the normalized SIFs $F_I = K_I/\sigma\sqrt{\pi a}$, $F_{II} = K_{II}/\sigma\sqrt{\pi a}$ are plotted against various material combinations and relative crack lengths in Figure 7. The solid lines denote the SIFs for the case of bending loading conditions and the dashed lines are those for tensile loading conditions which were computed in the previous research (Noda *et al.*, 2010; Lan *et al.*, 2011b). As can be seen from these figures, the double logarithmic distributions behave good linear relationships when $a/W < 0.01$. Furthermore, the sign of slope for each

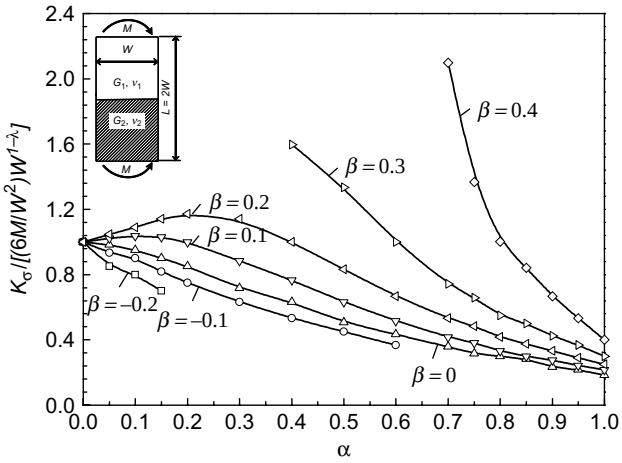

Figure 6.
Normalized intensity of stress singularity K_σ for various material combinations

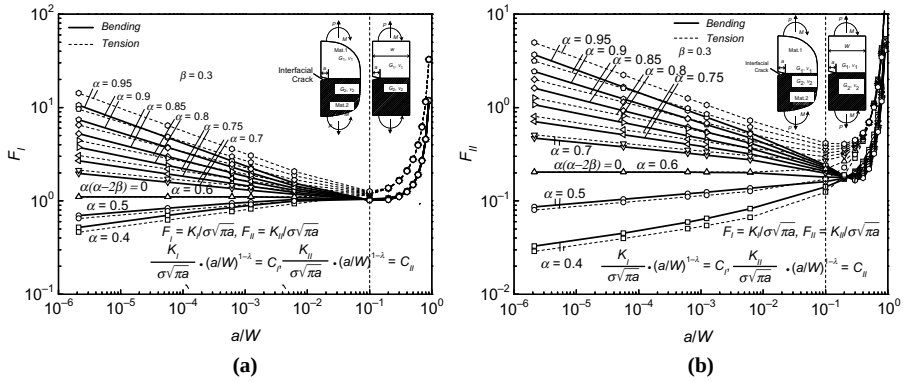

Figure 7.
Double logarithmic distributions of (a) F_I and (b) F_{II} with relative crack length a/W

curve varies depending on the sign of $\alpha(\alpha - 2\beta)$. Specifically, the slope is positive when $\alpha(\alpha - 2\beta) < 0$, is zero when $\alpha(\alpha - 2\beta) = 0$ and is negative when $\alpha(\alpha - 2\beta) > 0$. Thus, it can be deduced for the limiting case, the normalized SIF values of $F_I = K_I/\sigma\sqrt{\pi a}$, $F_{II} = K_{II}/\sigma\sqrt{\pi a}$ for the bonded semi-infinite plate ($a/W \to 0$) take the form:

$$\begin{aligned} &\alpha(\alpha - 2\beta) > 0: \quad F_I, F_{II} \to \infty \\ &\alpha(\alpha - 2\beta) = 0: \quad F_I, F_{II} \to \textit{finite} \\ &\alpha(\alpha - 2\beta) < 0: \quad F_I, F_{II} \to 0 \end{aligned} \tag{24}$$

By comparing the values of the two loading conditions for the shallow edge cracks near the interface corner, it can be found that they coincide very good when $\alpha(\alpha - 2\beta) = 0$. Furthermore, the SIFs for the bending loading conditions are smaller than those for the tensile case when $\alpha(\alpha - 2\beta) > 0$. In contrary, they are larger than those for the tensile case when $\alpha(\alpha - 2\beta) < 0$.

4.3 Asymptotic expressions for the SIFs of a shallow edge interface crack in a bonded strip under bending

In the above section, it has been proved that the normalized SIFs F_I,F_{II} have finite non-zero values only when $\alpha(\alpha - 2\beta) = 0$. In Figure 8, F_I, F_{II} for an edge interface crack in a bonded semi-infinite plates for $\alpha = 2\beta$ are plotted. From the figure, it is clear that F_I and F_{II} behave quadratic and linear relationship, respectively. The computed results for $\alpha = 2\beta$ are also tabulated in Table IV. Then, the approximate expression as in equation (26) is given by fitting the computed results. In equation (26), the result for the homogenous semi-infinite plate (materials are identical $\alpha = \beta = 0$) is $K_I/\sigma\sqrt{\pi a} = 1.121$, and it has an error of 0.062 per cent comparing with the famous theoretical one $K_I/\sigma\sqrt{\pi a} = 1.1215$.

$$\begin{aligned} K_I/\sigma\sqrt{\pi a} &= 1.121 + 0.0159\beta - 0.221\beta^2 \\ K_{II}/\sigma\sqrt{\pi a} &= -0.684\beta \end{aligned} \tag{25}$$

The limiting solutions $a/W \to 0$ are controlled by the singular behavior of perfectly bonded strip (Noda *et al.*, 2010; Lan *et al.*, 2011b). As discussed in the section 4.1, the intensity of singular stress is proportional to the $W^{1-\lambda}$. So, we plot the results of $F_I \cdot (W/a)^{1-\lambda}$ and $F_{II} \cdot (W/a)^{1-\lambda}$ against logarithmic relative crack length a/W in Figure 9(a) and (b), respectively. The material composite parameter β in Figure 9 is restricted to $\beta = 0.3$, but similar phenomenon can be found from other material combinations. As can be seen from these figures, the values for a given material combination approach to a constant with more than three-digits when $a/W < 10^{-2}$.

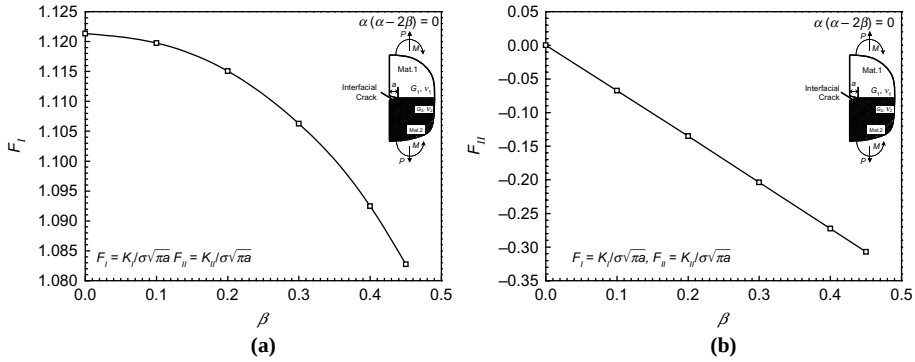

Figure 8.
Normalized SIFs (a) $F_I = K_I/\sigma\sqrt{\pi a}$ and (b) $F_{II} = K_{II}/\sigma\sqrt{\pi a}$ for $\alpha = 2\beta$ of an edge interface crack in a bonded semi-infinite plate

β	$K_I/\sigma\sqrt{\pi a}$	$K_{II}/\sigma\sqrt{\pi a}$
0	1.121	0
0.1	1.120	− 0.067
0.2	1.115	− 0.135
0.3	1.106	− 0.204
0.4	1.092	− 0.273
0.45	1.083	− 0.307

Table IV.
Results of the dimensionless SIFs for $\alpha = 2\beta$

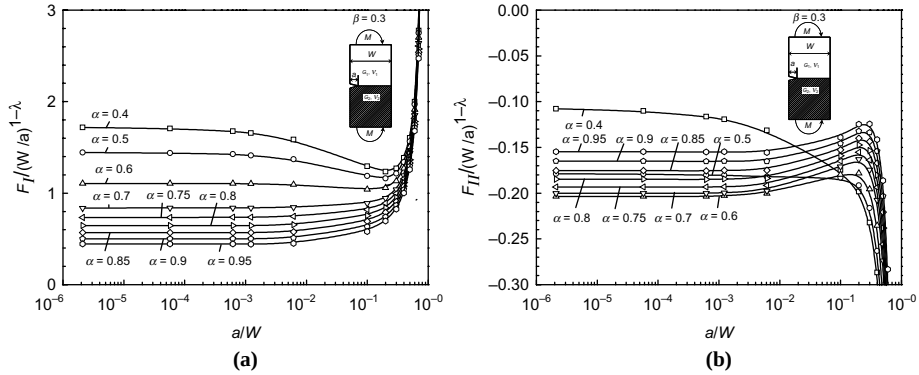

Figure 9.
Variations of (a) $F_I \cdot (W/a)^{1-\lambda}$ and (b) $F_{II} \cdot (W/a)^{1-\lambda}$ with relative crack length

Thus, we propose the following formula to calculate the SIFs at the crack tip for the shallow edge interface cracks in a bonded strip subjected to bending loading conditions.

$$\frac{K_I}{\sigma\sqrt{\pi a}} \cdot (a/W)^{1-\lambda} = C_I, \quad \frac{K_{II}}{\sigma\sqrt{\pi a}} \cdot (a/W)^{1-\lambda} = C_{II} \tag{26}$$

In equation (27), C_I, C_{II} are constants depending upon the elastic properties of materials. The results for the coefficients C_I, C_{II} are plotted and listed against material composite parameters in Figure 10(a) and Table V as well as in Figure 10(b) and Table VI, respectively. The dashed lines in Figure 10(a) and (b) are those for the tensile loading conditions (Noda *et al.*, 2010). It is easy to be found that the coefficient curves C_I, C_{II} in Figure 10 are the same for the two different loading conditions when $\alpha(\alpha - 2\beta) = 0$.

In conclusion, the solution of SIFs at the interface crack tip for a bonded dissimilar semi-infinite plate takes the following form:

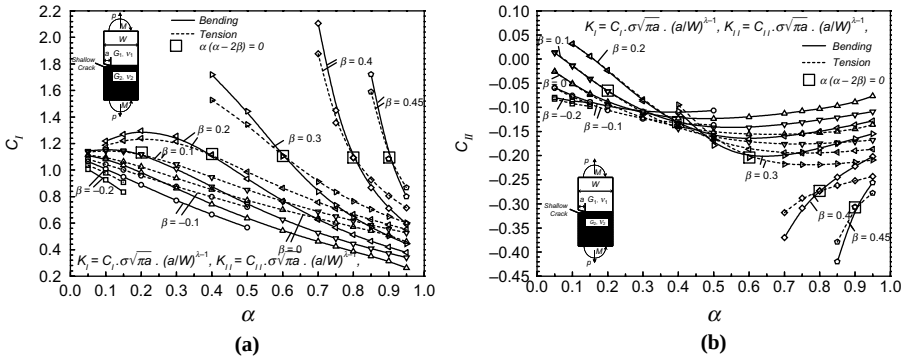

Figure 10.
Constants (a) C_I and (b) C_{II}

α	β = −0.2	β = −0.1	β = 0	β = 0.1	β = 0.2	β = 0.3	β = 0.4	β = 0.45
0.05	1.004	1.065	1.109	1.143	–			
0.1	0.925	1.009	1.081	1.157	1.219			
0.15	0.833	0.949	1.037	1.148	1.269			
0.2		0.888	0.982	1.120	1.295			
0.3		0.77	0.861	1.011	1.257			
0.4		0.664	0.742	0.875	1.115	1.718		
0.5		0.566	0.636	0.743	0.934	1.443		
0.6			0.542	0.627	0.766	1.106		
0.7			0.461	0.528	0.626	0.838	2.106	
0.75			0.423	0.485	0.566	0.734	1.45	
0.8			0.387	0.445	0.512	0.644	1.092	
0.85			0.351	0.408	0.463	0.568	0.867	1.72
0.9			0.312	0.373	0.419	0.502	0.711	1.083
0.95			0.262	0.341	0.379	0.445	0.594	0.799

Table V.
Tabulated values of C_I

α	β = −0.2	β = −0.1	β = 0	β = 0.1	β = 0.2	β = 0.3	β = 0.4	β = 0.45
0.05	−0.080	−0.059	−0.026	0.013	–			
0.1	−0.087	−0.076	−0.051	−0.014	0.032			
0.15	−0.090	−0.089	−0.072	−0.041	0.006			
0.2		−0.098	−0.089	−0.067	−0.024			
0.3		−0.109	−0.113	−0.109	−0.087			
0.4		−0.111	−0.123	−0.133	−0.135	−0.108		
0.5		−0.107	−0.124	−0.142	−0.160	−0.179		
0.6			−0.120	−0.142	−0.166	−0.204		
0.7			−0.113	−0.135	−0.160	−0.200	−0.370	
0.75			−0.108	−0.131	−0.155	−0.193	−0.309	
0.8			−0.103	−0.126	−0.150	−0.185	−0.273	
0.85			−0.097	−0.121	−0.143	−0.175	−0.245	−0.420
0.9			−0.089	−0.115	−0.136	−0.165	−0.222	−0.307
0.95			−0.077	−0.109	−0.128	−0.155	−0.202	−0.256

Table VI.
Tabulated values of C_{II}

$$\begin{cases} \dfrac{K_I}{\sigma\sqrt{\pi a}} = 1.121 + 0.0159\beta - 0.221\beta^2, & \dfrac{K_{II}}{\sigma\sqrt{\pi a}} = -0.684\beta when \alpha(\alpha - 2\beta) = 0; \\ \frac{K_I}{\sigma\sqrt{\pi a}}(a/W)^{1-\lambda} = C_I, \quad \frac{K_{II}}{\sigma\sqrt{\pi a}}(a/W)^{1-\lambda} = C_{II} \ \ when \ \ \alpha(\alpha - 2\beta) \neq 0. \end{cases} \tag{27}$$

5. Conclusions

In this paper, a single-edge cracked bonded strips subjected to the bending loading conditions were analyzed with varying the relative crack length and material combinations systematically. The SIFs of interface crack were evaluated by using the ratio of crack-tip stress values between the reference and target unknown problems. In order to obtain the high accurate SIFs without using very fine mesh pattern in FE model, the extrapolated technique was proposed and examined by using the results of two different meshes. The limiting solutions for a dissimilar bonded semi-infinite plates ($a/W \rightarrow 0$) under bending were also provided and compared with that of tensile loading case. Specifically, since a linear relationship between $F_I \cdot (W/a)^{1-\lambda}$, $F_{II} \cdot (W/a)^{1-\lambda}$ and the relative crack length a/W was observed for the shallow edge crack case in Figure 9, the SIFs for an edge interface crack in bonded semi-infinite plates can be expressed as:

$$\begin{cases} \dfrac{K_I}{\sigma\sqrt{\pi a}} = 1.121 + 0.0159\beta - 0.221\beta^2, & \dfrac{K_{II}}{\sigma\sqrt{\pi a}} = -0.684\beta \ \ when \ \ \alpha(\alpha - 2\beta) = 0; \\ \frac{K_I}{\sigma\sqrt{\pi a}}(a/W)^{1-\lambda} = C_I, \quad \frac{K_{II}}{\sigma\sqrt{\pi a}}(a/W)^{1-\lambda} = C_{II} \ \ when \ \ \alpha(\alpha - 2\beta) \neq 0. \end{cases}$$

References

Akisanya, N.A. and Fleck, N.A. (1997), "Interfacial cracking from the free-edge of a long bi-material strip", *Int. J. Solids Struct.*, Vol. 34, pp. 1645-65.

Bogy, D.B. (1968), "Edge-bonded dissimilar orthogonal elastic wedges under normal and shear loading", *Trans. ASME, J. Appl. Mech.*, Vol. 35, pp. 460-6.

Bogy, D.B. (1971), "Two edge-bonded elastic wedges of different materials and wedges angles under surface tractions", *J. Appl. Mech.*, Vol. 38, pp. 377-86.

Bogy, D.B. and Wang, K.C. (1971), "Stress singularities at interface corners in bonded dissimilar isotropic elastic materials", *Int. J. Solids, Struct.*, Vol. 7, pp. 993-1005.

Chen, D. and Nishitani, H. (1993), "Intensity of singular stress field near the interface edge point of a bonded strip", *Trans. JSME*, Vol. 59, pp. 2682-6.

Dempsey, J.P. and Sinclair, G.B. (1979), "On the stress singularities in the plane elasticity of the composite wedge", *J. Elast.*, Vol. 9, pp. 373-91.

Dong, Y.X., Wang, Z.M. and Wang, B. (1997), "On the computation of stress intensity factors for interfacial cracks using quarter point boundary elements", *Eng. Fract. Mech.*, Vol. 57, pp. 335-42.

Erdogan, F. (1965), "Stress distribution in bonded dissimilar materials with cracks", *Trans. ASME, J. Appl. Mech.*, Vol. 32, pp. 403-10.

Hein, V.L. and Erdogan, F. (1971), "Stress singularities in a two-material wedge", *Int. J. of Fract. Mech.*, Vol. 7, pp. 317-30.

Kakuno, H., Oda, K. and Morisaki, T. (2010), "Analysis of stress intensity factor for interface crack in bonded dissimilar plate under bending", *Key Engineering Materials*, Vol. 417/418, pp. 153-6.

Lan, X., Noda, N.A., Michinaka, K. and Zhang, Y. (2011a), "The effect of material combinations and relative crack size to the stress intensity factors at the crack tip of a bi-material bonded strip", *Eng. Fract. Mech.*, Vol. 78, pp. 2572-84.

Lan, X., Noda, N.A., Zhang, Y. and Michinaka, K. (2011b), "Single and double edge interface crack solutions under arbitrary material combinations", *Acta Mechanica Solida Sinica*, Vol. 25 No. 4, pp. 404-16.

Liu, Y.H., Wu, Z.G., Liang, Y.C. and Liu, X.M. (2008), "Numerical methods for determination of stress intensity factors of singular stress field", *Eng. Fract. Mech.*, Vol. 75, pp. 4793-803.

Matsumto, T., Tanaka, M. and Obara, R. (2000), "Computation of stress intensity factors of interface cracks based on interaction energy release rates and BEM sensitivity analysis", *Eng. Fract. Mech.*, Vol. 65 No. 6, pp. 683-702.

Miyazaki, N., Ikeda, T., Soda, T. and Munakata, T. (1993), "Stress intensity factor analysis of interface crack using boundary element method – application of contour-integral method", *Eng. Fract. Mech.*, Vol. 45 No. 5, pp. 599-610.

Nisitani, H., Kawamura, T., Fujisaki, W. and Fukuda, T. (1999), "Determination of highly accurate values of stress intensity factor or stress concentration factor of plate specimen by FEM", *Transactions of the Japan Society of Mechanical Engineers, Series A*, Vol. 65 No. 629, pp. 26-31 (in Japanese).

Noda, N.A., Lan, X., Michinaka, K., Zhang, Y. and Oda, K. (2010), "Stress intensity factor of an edge interface crack in a bonded semi-infinite plate", *Trans. JSME, Series A*, Vol. 76 No. 770, pp. 1270-7 (in Japanese).

Oda, K., Kamisugi, K. and Noda, N.-A. (2009), "Analysis of stress intensity factor for interface cracks based on proportional method", *Transactions of the Japan Society of Mechanical Engineers, Series A*, Vol. 75 No. 752, pp. 476-782 (in Japanese).

Reedy, E.D. Jr and Guess, T.R. (1993), "Composite to metal tubular lap joints: strength and fatigue resistance", *Int. J. Fract.*, Vol. 63, pp. 351-67.

Treifi, M., Oyadiji, S.O. and Tsang, D.K.L. (2008), "Computations of modes I and II stress intensity factors of sharp notched plates under in-plane shear and bending loading by the fractal-like finite element method", *Int. J. Solids Struct.*, Vol. 45, pp. 6468-84.

Treifi, M., Oyadiji, S.O. and Tsang, D.K.L. (2009), "Computations of the stress intensity factors of double-edge and centre V-notched plates under tension and anti-plane shear by the fractal-like finite element method", *Eng. Fract. Mech.*, Vol. 76, pp. 2091-108.

Van Vroonhoven, J.C.W. (1992), "Stress singularities in bi-material wedges with adhesion and delamination", *Fatigue & Fracture of Enginnering Mater. & Struct.*, Vol. 15, pp. 157-71.

Wu, Y.L. (1994), "A new method for evaluation of stress intensities for interface cracks", *Eng. Fract. Mech.*, Vol. 48, pp. 755-61.

Xu, J.-Q., Liu, Y.-H. and Wang, X.-G. (1999), "Numerical methods for the determination of multiple stress singularities and related stress intensity coefficients", *Eng. Fract. Mech.*, Vol. 63, pp. 775-90.

Xuan, Z.C., Feng, Z.S. and Gao, D.Y. (2007), "Computing lower and upper bounds on stress intensity factors in bimaterials", *Int. J. Non-Linear Mech.*, Vol. 42 No. 2, pp. 336-41.

Yang, X.X. and Kuang, Z.B. (1996), "Contour integral method for stress intensity factors of interface crack", *Int. J. Fract.*, Vol. 78, pp. 299-313.

Yuuki, R. and Cho, S.B. (1989), "Efficient boundary element analysis of stress intensity factors for interface cracks in dissimilar materials", *Eng. Fract. Mech.*, Vol. 34, pp. 179-88.

Further reading

Williams, M.L. (1952), "Stress singularities resulting from various boundary conditions in angular corners of plates in extension", *J. Appl. Mech.*, Vol. 19, pp. 526-8.

Corresponding author

Xin Lan can be contacted at: xinlan_al@yahoo.com